CHEMISTRY
A EUROPEAN JOURNAL

DOI: 10.1002/chem.201000849

The Conformational Landscape of Nicotinoids: Solving the Conformational Disparity of Anabasine

Alberto Lesarri,*[a] Emilio J. Cocinero,[b] Luca Evangelisti,[c] Richard D. Suenram,[d] Walther Caminati,[c] and Jens-Uwe Grabow[e]

Abstract: The conformational landscape of the alkaloid anabasine (neonicotine) has been investigated by using rotational spectroscopy and ab initio calculations. The results allow a detailed comparison of the structural properties of the prototype piperidinic and pyrrolidinic nicotinoids (anabasine vs. nicotine). Anabasine adopts two most stable conformations in isolation conditions, for which we determined accurate rotational and nuclear quadrupole coupling parameters. The preferred conformations are characterized by an equatorial pyridine moiety and additional N–H equatorial stereochemistry at the piperidine ring (eq-eq; eq = equatorial). The two rings of anabasine are close to a bisecting arrangement, with the observed conformations differing by an approximately 180° rotation of the pyridine subunit, denoted either *syn* or *anti*. The preference of anabasine for the eq-eq-*syn* conformation has been established by relative intensity measurements (*syn*/*anti* ~ 5(2)). The conformational preferences of free anabasine are directed by a weak N···H–C hydrogen bond interaction between the nitrogen lone pair at piperidine and the closest C–H bond in pyridine, with N···H distances ranging from 2.686 (*syn*) to 2.667 Å (*anti*). Supporting ab initio calculations by using MP2 and the recent M05-2X density functional are provided, evaluating the predictive performance of both methods.

Keywords: alkaloids · conformation analysis · nicotinoids · rotational spectroscopy · stereochemistry

Introduction

The nicotinoids are alkaloids sharing a two-ring assembly with a 3-pyridyl methylamine skeleton. The structural prototype of pyrrolidinic nicotinoids is nicotine (1-methyl-2-(3-pyridyl)pyrrolidine), which has been thoroughly investigated in connection with its role as an agonist of the acetylcholine receptor (nAChR).[1] Understanding the mechanisms of molecular recognition in nAChR is crucial for the design of novel agonists targeting not only nicotine addiction but also disorders in the central nervous system, such as Alzheimer or schizophrenia.[2]

Two pharmacophores have been recognized in acetylcholine (ACh), a nonbonding electron pair providing hydrogen bonding to the receptor and a positively charged nitrogen center responsible for a cation-π interaction.[1,3] Ionized nicotine mimics ACh, but the N···N distance between the recognition sites is conformer-dependent. In consequence, the investigation of the intrinsic conformational preferences in nicotine is biochemically relevant and has been targeted with different techniques. The gas electron diffraction was studied by Konaka[4] who reported two dominant conformers with an equatorial pyridine roughly bisecting pyrrolidine. The microwave spectrum of nicotine was studied by Lavrich

[a] Prof. Dr. A. Lesarri
Departamento de Química Física y Química Inorgánica
Universidad de Valladolid
47011 Valladolid (Spain)
Fax: (+34) 983-423013
E-mail: lesarri@qf.uva.es
Homepage: http://www.uva.es/lesarri

[b] Dr. E. J. Cocinero
Departamento de Química Física
Universidad del País Vasco, Ap. 644
48080 Bilbao (Spain)

[c] L. Evangelisti, Prof. Dr. W. Caminati
Dipartimento di Chimica "G.Ciamician" dell'Università
Via Selmi 2, 40126 Bologna (Italy)

[d] Dr. R. D. Suenram
Department of Chemistry
University of Virginia, McCormick Rd.
Charlottesville, Virginia 22904 (USA)

[e] Prof. Dr. J.-U. Grabow
Institut für Physikalische Chemie & Elektrochemie
Lehrgebiet A, Gottfried-Wilhelm-Leibniz-Universität
Callinstrasse 3 A, 30167 Hannover (Germany)

Supporting information for this article is available on the WWW under http://dx.doi.org/10.1002/chem.201000849.

View this journal online at wileyonlinelibrary.com

© 2010 Wiley-VCH Verlag GmbH & Co. KGaA, Weinheim

and Suenram and revealed the same two conformations.[5] Several theoretical calculations have also been reported.[6]

Piperidinic nicotinoids can also act as agonists of nAChR. However, unlike nicotine, the structural information on these nicotinoids is scarce. X-ray diffraction studies[7] on the prototypical anabasine (neonicotine, 2-(3-pyridil)piperidine) showed consensus on the piperidinic chair motif, but explicitly reported a "substantial conformational disparity" concerning the orientation of its pyridine moiety. Since there were no previous experimental investigations on the intrinsic structure of the free molecule the absence of solvent, matrix, or crystal effects, the question remained unsolved. Additionally, the structural properties of the free molecule are crucial to validate the predictive power of theoretical methods, either molecular mechanics used in large-scale simulations or the more accurate density functional or ab initio calculations. For all these reasons we investigated anabasine by using Fourier-transform microwave (FTMW) spectroscopy in a supersonic jet.[8] The use of an adiabatic supersonic expansion provides a virtually collisionless environment, freezing the different conformers in their vibrational ground states and populating only the lowest rotational quantum numbers. Furthermore, the inherent high resolution of microwave spectroscopy (linewidths <10 kHz) allows the discrimination of all plausible conformers or even isotopologues, with no other prerequisite than a permanent dipole moment.

The experiment was assisted by several ab initio calculations interrogating not only the spectroscopic parameters relevant for the interpretation of the jet-cooled spectra, but also the conformational landscape and feasible relaxation pathways that might reduce the number of detectable species by interconversion to lower-energy forms.

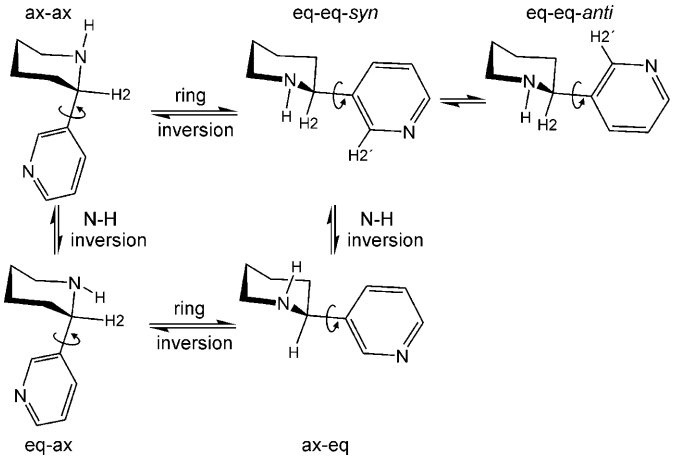

Scheme 1. Plausible conformations of anabasine.

Results: Rotational Spectrum and Structure

Assuming that saturated six-membered rings adopt a chair conformation, the elucidation of the structure of anabasine requires considering the stereochemistry at the piperidine nitrogen atom (axial (ax)/equatorial (eq)), the pyridil position in piperidine (axial/equatorial), and the rotamerization of the pyridil ring. If, as observed in nicotine,[4–6] the pyridine ring was attached nearly bisecting piperidine, two preferred orientations separated by an approximately 180° internal rotation (*syn*/*anti* attending to H2/H2′) could be anticipated. In consequence, the $2^3=8$ conformations of Scheme 1 could be expected for anabasine and would produce distinct rotational signatures.

Following model calculations of the rotational constants (A, B, C) for the plausible structures, a survey of the microwave spectrum immediately identified the intense lines of the most abundant conformation. The spectrum was assigned on the basis of a series of μ_a R-branch ($J+1\leftarrow J$) rotational transitions appearing at $(B+C)\approx 990$ MHz intervals, characteristic of near-prolate asymmetric rotors. A set of additional μ_b transitions was assigned later, finally covering angular momentum quantum numbers $J=3$–19. In further frequency scans the weaker transitions of a second conformer could be positively identified, for which transitions with μ_a and μ_b selection rules ($J=3$–13) were measured similarly. No other conformations were detected in the jet-cooled expansion.

As exemplified in Figure 1, all transitions exhibit very complex hyperfine patterns, typically splitting each transition into nine more intense components spread less than 500 kHz, which would not be resolvable with any kind of vibrational or electronic spectroscopies. The hyperfine effects were accounted for in terms of the interaction between the electric quadrupole of the two ^{14}N ($I=1$) nuclei and the molecular electric field gradient, coupling the nuclear spins to the overall rotation ($\boldsymbol{I}=\boldsymbol{I}_1+\boldsymbol{I}_2$, $\boldsymbol{F}=\boldsymbol{I}+\boldsymbol{J}$).[9,10] As shown in

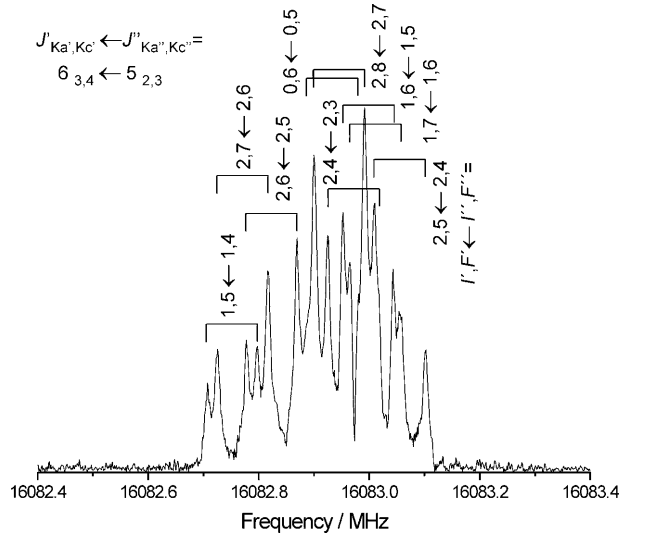

Figure 1. The $6_{3,4}\leftarrow 5_{2,3}$ rotational transition of eq-eq-*syn* anabasine illustrates the complex hyperfine patterns arising from the two-nuclei ^{14}N nuclear quadrupole coupling (hyperfine components labelled as $I',F'\leftarrow I'',F''$; $\boldsymbol{I}=\boldsymbol{I}_1+\boldsymbol{I}_2$, $\boldsymbol{F}=\boldsymbol{I}+\boldsymbol{J}$) . All component lines appear as a doublet from the Doppler Effect.

 © 2010 Wiley-VCH Verlag GmbH & Co. KGaA, Weinheim

Table 1, the analysis of the observed transitions by using the Watson's semirigid rotor Hamiltonian[11] (S-reduction) rendered accurate rotational and centrifugal distortion constants and the nuclear quadrupole coupling parameters for the two observed conformers of anabasine. Off-diagonal nuclear quadrupole coupling contributions were not required to fit the observed transitions to experimental accuracy ($\sigma <$ 2 kHz). The set of measured rotational transitions and residuals is given in the Supporting Information as Tables S1 and S2.

Table 1. Rotational parameters of anabasine and comparison with the ab initio predictions by using MP2 and DFT theory (M05-2X functional).

	Experiment		Theory MP2 [M05-2X]	
	eq-eq-*syn*	eq-eq-*anti*	eq-eq-*syn*	eq-eq-*anti*
A [MHz][a]	2523.91921(18)[d]	2505.84766(32)	2520.1 [2545.6]	2501.3 [2529.6]
B [MHz]	505.16717(16)	509.00907(15)	504.8 [508.9]	507.7 [510.3]
C [MHz]	485.22787(12)	486.45464 (14)	487.24 [489.4]	489.5 [492.8]
D_J [kHz]	0.012569(50)	0.01363(42)	0.010 [0.011]	0.011 [0.013]
D_{JK} [kHz]	0.0897(12)	0.0741(15)	0.089 [0.087]	0.082 [0.085]
D_K [kHz]	0.075(12)	0.127(16)	0.070 [0.078]	0.086 [0.085]
d_1 [Hz]	−1.15(10)	0.00[e]	−0.59[−0.74]	−0.29[−0.25]
d_2 [Hz]	−2.664(47)	−3.270(82)	−1.76[−1.97]	−1.98[−2.56]
^{14}N1′				
χ_{aa} [MHz]	−0.9731(48)	0.764(10)	−0.96[−1.10]	0.83 [0.84]
χ_{bb} [MHz]	−0.331(26)	−1.552(33)	−0.37[−0.39]	−1.49[−1.47]
χ_{cc} [MHz]	1.305(26)	0.788(33)	1.32 [1.50]	0.66 [0.63]
^{14}N1				
χ_{aa} [MHz]	2.46198(43)	2.4920(93)	2.49 [2.69]	2.48 [2.67]
χ_{bb} [MHz]	0.403(24)	0.254(31)	0.15 [0.42]	0.10 [0.22]
χ_{cc} [MHz]	−2.865(24)	−2.746(31)	−2.64[−3.11]	−2.58[−2.89]
$\lvert\mu_a\rvert$ [D]			2.21 [2.25]	1.52 [1.55]
$\lvert\mu_b\rvert$ [D]			1.05 [1.07]	2.16 [2.13]
$\lvert\mu_c\rvert$ [D]			0.37 [0.35]	1.99 [2.04]
$\lvert\mu_{TOT}\rvert$ [D]			2.47 [2.51]	3.30 [3.33]
N[b]	124	106		
σ [kHz]	1.7	2.0		
ΔE [kJ mol^{-1}][c]			0.0	3.1 [2.7]
ΔG^{333} [kJ mol^{-1}]			0.0	3.0 [2.4]

[a] Rotational constants (A, B, C); Watson's quartic centrifugal distortion constants (D_J, D_{JK}, D_K, d_1, d_2); Nuclear quadrupole coupling tensor elements ($\chi_{\alpha\beta}$, α, β = a, b, c) for the pyridine and piperidine ^{14}N atoms and electric dipole moment components (μ_α, α = a, b, c; 1 D ≈ 3.336×10^{-3} C m) referred to the principal inertial axis. [b] Number of transitions (N) and rms deviation (σ) of the fit. [c] Relative energies with respect to the global minimum (zero-point-energy corrected) and Gibbs free energies at 333 K and 1 atm. [d] Standard error in parentheses in units of the last digit. [e] Fixed to zero.

An unequivocal conformational assignment was established by comparison of the experimental rotational constants and the nuclear quadrupole coupling parameters with their ab initio modeled values (also shown in Table 1). The ab initio calculations suggested that the eq-eq-*syn* (global minimum) and eq-eq-*anti* conformations in Scheme 1 would correspond to the most stable structures of anabasine. Accordingly, we found a very good agreement between the experimental parameters of the most populated conformer and those predicted for the global minimum eq-eq-*syn*. Similarly, the parameters determined for the less abundant conformer matched very well with the predictions for the eq-eq-*anti* species, calculated 3.1 kJ mol^{-1} above the global minimum. The observation of two conformations in anabasine is consistent with the large interconversion barrier (18.1 kJ mol^{-1}) predicted ab initio in Figure 2, which excludes a conformational relaxation between these conformers in the seeded expansion. All other anabasine conformations were predicted to be much higher in energy (> 13 (MP2) or > 9 kJ mol^{-1} (M05-2X) in Tables S3–S4 of the Supporting Information) and unequivocally discarded on the basis of the rotational and nuclear quadrupole coupling parameters, both extremely sensitive to the molecular geometry. The population ratio in the jet was estimated as eq-eq-*syn*/eq-eq-*anti* ~ 5(2) by using relative intensity measurements[12] and the theoretical dipole moments of Table 1. The preference of anabasine for the eq-eq-*syn* conformation is consistent with the ab initio Gibbs free energy difference of 3.0 kJ mol^{-1} (MP2) at 333 K, corresponding to an equilibrium population ratio of 3.4:1.

The intensity of the spectrum prevented at this moment the analysis of minor isotopic species in natural abundance.

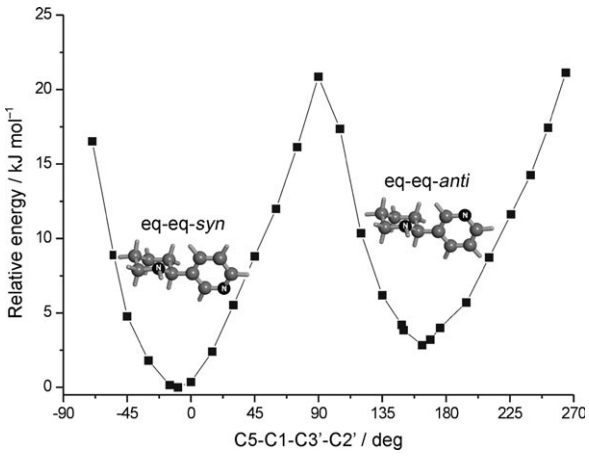

Figure 2. The ab initio (MP2/6-311++G(d,p)) potential curve for interconversion between the eq-eq-*syn* (global minimum) and eq-eq-*anti* conformers of anabasine.

 © 2010 Wiley-VCH Verlag GmbH & Co. KGaA, Weinheim

However, relevant structural information can be extracted from the rotational constants of the parent eq-eq-*syn* and eq-eq-*anti* species. To this purpose, we fitted three structural parameters defining the orientation of the pyridine ring while keeping the rest of the molecule at the MP2 ab initio predicted configuration (the M05-2X behavior in Table 1 was clearly less dependable in terms of the rotational and hyperfine parameters). The most significant structural features observed in Figure 3 include a tilt of approximately

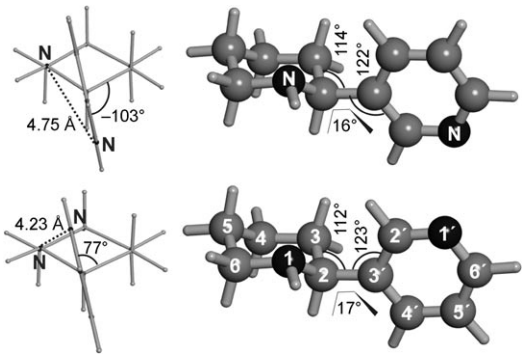

Figure 3. Intrinsic conformations of free anabasine detected by rotational spectroscopy: eq-eq-*syn* (top) and eq-eq-*anti* (bottom).

16–17° of the pyridine plane with respect to the ideal *syn* or *anti* configurations (C2′-C3′-C2-C3 = −103.1° in eq-eq-*syn* or +77.2° in eq-eq-*anti*). The two observed conformers differ practically in a 180° rotamerization, and the distances between the two nitrogen nuclei N···N range from 4.750 (eq-eq-*syn*) to 4.233 Å (eq-eq-*anti*). The effective structures are reported in Table 2 and reproduce the observed ground-state rotational constants below 1 MHz.

Discussion

We present the first experimental study of a piperidinic nicotinoid with rotational resolution, resolving its complicated nuclear quadrupole coupling hyperfine effects and establishing its intrinsic conformational and spectroscopic properties in the ground state. The preference of the planar pyridine ring towards an orientation equatorial to the piperidine chair is unequivocally confirmed, together with the equatorial *N*-methyl stereochemistry of piperidine. The rotamerization of pyridine results in two most stable *syn*/*anti* conformations for the free molecule, virtually identical in the orientation of the pyridine ring. The deviation of the observed conformers with respect to the ideal *syn*/*anti* orientation of 16–17° is noticeable, most probably reflecting a weak N···H–C hydrogen bond interaction between the nitrogen lone pair of piperidine and the closest hydrogen atom in pyridine, either H4′ (*syn*) or H2′ (*anti*). The N···H distances of 2.686 (*syn*) or 2.667 Å (*anti*) are within the 2.5–2.7 Å range for these weak interactions.[13,14,15]

Table 2. Effective structures of anabasine in the gas phase. The fitted parameters are shown in bold, with the rest of the structural parameters constrained to the MP2/6-311++G(d,p) near-equilibrium ab initio values. The values in parenthesis show the starting ab initio values. Notation after Figure 3 (hydrogen atoms omitted).

	eq-eq-*syn*[a] r_0	eq-eq-*anti* r_0
$r(N_1–C_6)$	1.467	1.466
$r(C_6–C_5)$	1.526	1.526
$r(C_5–C_4)$	1.531	1.531
$r(C_4–C_3)$	1.531	1.531
$r(C_3–C_2)$	1.534	1.534
$r(C_2–C_3')$	1.505	1.506
$r(C_3'–C_2')$	1.402	1.406
$r(C_2'–N_1')$	1.345	1.345
$r(N_1'–C_6')$	1.345	1.346
$r(C_6'–C_5')$	1.400	1.399
$r(C_5'–C_4')$	1.396	1.397
$<(C_5\text{-}C_6\text{-}N_1)$	109.35	109.28
$<(C_4\text{-}C_5\text{-}C_6)$	110.11	110.11
$<(C_3\text{-}C_4\text{-}C_5)$	110.26	110.31
$<(C_2\text{-}C_3\text{-}C_4)$	110.68	110.63
$<(C_3'\text{-}C_2\text{-}C_3)$	**113.68**(111.24)	**111.56**(111.32)
$<(C_2'\text{-}C_3'\text{-}C_2)$	**121.93**(120.98)	**122.9**(120.68)
$<(N_1'\text{-}C_2'\text{-}C_3')$	124.54	124.19
$<(C_6'\text{-}N_1'\text{-}C_2')$	116.67	116.97
$<(C_5'\text{-}C_6'\text{-}N_1')$	123.57	123.61
$<(C_4'\text{-}C_5'\text{-}C_6')$	118.89	118.58
$\tau(C_4\text{-}C_5\text{-}C_6\text{-}N_1)$	57.91	57.90
$\tau(C_3\text{-}C_4\text{-}C_5\text{-}C_6)$	−54.12	−54.06
$\tau(C_2\text{-}C_3\text{-}C_4\text{-}C_5)$	54.17	54.11
$\tau(C_3'\text{-}C_2\text{-}C_3\text{-}C_4)$	−178.39	−178.67
$\tau(C_2'\text{-}C_3'\text{-}C_2\text{-}C_3)$	**−103.14**(−104.51)	**77.18**(74.17)
$\tau(C_1'\text{-}C_2'\text{-}C_3'\text{-}C_2)$	177.05	−178.38
$\tau(C_6'\text{-}C_1'\text{-}C_2'\text{-}C_3')$	1.74	0.28
$\tau(C_5'\text{-}C_6'\text{-}C_1'\text{-}C_2')$	−1.07	−0.40
$\tau(C_4'\text{-}C_5'\text{-}C_6'\text{-}C_1')$	0.00	0.22

[a] Bond lengths [Å], valence angles [°], and dihedrals [°] are denoted *r*, <, and τ, respectively.

The observed conformations of anabasine can be rationalized in terms of the structure of related compounds. The preference of the chaired piperidine moiety for a N–H equatorial conformation is well established, as observed for the isolated molecule in piperidine,[16] tropinone,[17] and 1-methyl-4-piperidinone.[18] This preference was attributed in piperidine to the delocalization of the nitrogen lone pair and steric effects.[19] In our conformational search, the most stable N–H axial conformations (ax-eq in Scheme 1) were found at relative energies of 9 (M05)–13 kJ mol^{-1} (MP2) over the global minimum, so they are depopulated in the expansion. The conformational properties of six-membered two-ring assemblies were examined in a classical work of Eliel on phenylcyclohexanes.[20,21] Generally speaking a cyclohexane attached to a sp^2-hybridized group would tend to adopt a relative orientation with the substituent nearly perpendicular to the bisector plane of cyclohexane.[22] However, for phenylcyclohexane the perpendicular axial phenyl imposes large steric constraints between its *ortho* hydrogen atoms and the adjacent equatorial hydrogen atoms in cyclohexane, which are avoided in the bisecting equatorial conformation. The similarities[22,23] between piperidine and cy-

 © 2010 Wiley-VCH Verlag GmbH & Co. KGaA, Weinheim

clohexane make this explanation valid for anabasine also. The modulating role of the weak N···H–C intramolecular hydrogen bond in anabasine is supported by contrasting ab initio predictions on phenylcyclohexane in Tables S5–S6 (see the Supporting Information), which suggests an ideal bisecting orientation for the equatorial molecule. Whereas intramolecular hydrogen bonding is often masked in crystal structures, it is revealed as a decisive interaction in multiple biological molecules observed under isolation conditions, such as amino acids.[24] Interestingly, Eliel noticed that the introduction of a methyl group in 1-methyl-1-phenylcyclohexane would reverse the conformational equilibrium from bisecting equatorial to perpendicular axial, that is, rotating approximately 90° the orientation of the phenyl group.[20] The conformational search of anabasine also showed that the axial pyridine conformations (ax-ax and eq-ax) exhibits a near-perpendicular aromatic ring, but their large relative energies >13 (MP2)–12 kJ mol^{-1} (M05-X2) in Table S4 (see the Supporting Information) make them undetectable.

The striking differences between the free molecule and the crystal structures illustrate the importance of the gas-phase studies. The few known anabasinium salts[7] studied to date revealed only a single conformer (except in the *O*-*O*′-diethylphosphorothioate[25]), and the relative orientation between the two rings is widely changing in the crystal (i.e., differences of up to 33° in C_2'-C_3'-C_2-C_3 for eq-eq-*syn* or 44° for eq-eq-*anti* conformations). Further arguments would require the investigation of additional structures of anabasine, in particular, that of its crystal neutral form, which is available for nicotine[26] but unknown for anabasine. However, our new data confirm that the claim about "conformational disparity" in this molecule deduced from the X-ray diffraction data is purely a crystal packing effect.

Conversely, our study of the free molecule emphasizes the similarities with nicotine. In both compounds the eq-eq-*syn* conformation gives rise to the most stable conformer and the relative energy with the eq-eq-*anti* species is comparable (MP2: 3.1 in Table 1 vs. 2.4 kJ mol^{-1} in nicotine). Furthermore, both the orientation between the two rings (MP2: C_2'-C_3'-C_2-$C_3 = -107.7/72.3$° in nicotine) and the N···N distances (MP2: 4.800/4.242 Å in nicotine) are similar in the two molecules. In conclusion, the structural homology of anabasine and nicotine is confirmed from the study of the free molecules in the gas phase.

The experiment and the theoretical data generally compare satisfactory for this molecule, but the inferior behavior of the computationally effective M05-2X[27] empirical functional in this molecule with respect to the conventional MP2 approach is worth noting. The need for accurate DFT methods suitable for the investigation of large biomolecular systems will probably require not only assessment with other reference theoretical methods,[28] but also contrasting with rotational experiments, which provide an ultimate benchmark for molecular structure.

This work calls for additional high-resolution structural studies on anabasine and other nicotinoids, which are poorly covered in the literature. Additionally, it illustrates the value of rotational data and the benefits of modern microwave spectroscopy techniques, which are extending to larger systems and offer a valuable insight into the molecular properties, structure, and dynamics of biological building blocks.

Experimental Section

Experimental methods: The rotational spectrum was surveyed in the region of 6–26 GHz with the FTMW[8] spectrometer in Hannover.[29] Briefly, the sample is probed in a supersonic jet expansion expanded into a Fabry–Pérot microwave resonator, by using short (μs) excitation pulses at microwave frequencies. The exciting radiation brings the molecular ensemble into coherence, inducing a macroscopic polarization. The subsequent transient spontaneous emission or free-induced-decay is then detected in the MW region, downconverted to the radiofrequency region and digitized in the time-domain. Finally, a Fourier transformation yields the frequency-domain spectrum, from which the resonance frequencies of the rotational transitions are measured. The collinear arrangement of the supersonic jet and the resonator axis results in an instrumental Doppler doubling, with the rest frequencies corresponding to the average frequency of the two Doppler components. The accuracy of the frequency measurements is below 3 kHz. Transitions separated by more than typically 6 kHz are resolvable.

Anabasine is a liquid at room temperature (m.p. 9 °C), so it was vaporized in a heating nozzle[30] under mild conditions (60 °C) and diluted in a current of neon used as a carrier gas (stagnation pressures of ca. 2 bar).

Computational methods: Several ab initio calculations implemented in Gausssian 03[31] were tested in this work. In particular, we compared the results of frozen-core second-order Moller–Plesset (MP2) perturbation theory and density functional theory, by using the recent Truhlar's M05–2X functional[27] in combination with a standard triple-ζ 6–311++G(d,p) basis set. M05–2X is a highly-parametrized *meta*-hybrid empirical functional developed to account for dispersion interactions, which are often relevant in biological molecules. The ab initio calculations included a search of the conformational space of anabasine, the identification of the stationary points on the potential energy surface, and the calculation of the rotational and hyperfine parameters of the title compound. In a later stage, the relaxation path between the two most stable conformations of the molecule was investigated. The analysis of the vibrational frequencies used the two theoretical methods in the harmonic approximation. The centrifugal distortion constants were estimated from the harmonic force field. Finally, to compare anabasine with nicotine and phenylcyclohexane, the conformations of these molecules were fully optimised by using the same theoretical methods used for anabasine.

Acknowledgements

Financial support from the Deutsche Forschungsgemeinschaft (DFG), the Land Niedersachsen, the Spanish MICINN (CTQ2009-14364, Consolider-Ingenio 2010/CSD2007-00013, CGL2008-0641/CLI), and the JCyL (VA017A08) is gratefully acknowledged. We thank Dr. T. Mercero for discussions and the IZO-SGI (UPV-EHU) for computational resources. E.J.C. acknowledges the MICINN for a "Juan de la Cierva" contract.

[1] a) K. Brejc, W. J. van Dijk, R. V. Klaassen, M. Schuurmans, J. van der Oost, A. B. Smit, T. K. Sixma, *Nature* **2001**, *411*, 269; b) G. B. Wells, *Front. Biosci.* **2008**, *13*, 5479; c) V. Tsetlin, F. Hucho, *Curr. Opin. Pharmacol.* **2009**, *9*, 1.

[2] S. N. Haydar, C. Ghiron, L. Bettinetti, H. Bothmann, T. A. Comery, J. Dunlop, S. La Rosa, I. Micco, M. Pollastrini, J. Quinn, R. Roncarati, C. Scali, M. Valacchi, M. Varrone, R. Zanaletti, *Bio. Med. Chem.* **2009**, *17*, 5247.

 © 2010 Wiley-VCH Verlag GmbH & Co. KGaA, Weinheim

[3] D. L. Bene, G. S. Brandt, W. G. Zhong, N. M. Zacharias, H. A. Lester, D. A. Dougherty, *Biochemistery* **2002**, *41*, 10262.
[4] T. Takeshima, R. Fukumoto, T. Egawa, S. Konaka, *J. Phys. Chem. A* **2002**, *106*, 8734.
[5] R. J. Lavrich, R. D. Suenram, D. F. Plusquellic, S. Davis, 58th International Symposium on Molecular Spectroscopy (Columbus, OH), **2003**, Comm. RH13.
[6] a) M. Koné, B. Illien, C. Laurence, J.-F. Gal, P.-C. Maria, *J. Phys. Org. Chem.* **2006**, *19*, 104; b) J. Graton, M. Berthelot, J.-F. Gal, S. Girard, C. Laurence, J. Lebreton, J.-I. Le Questel, P.-C. Maria, P. Naus, *J. Am. Chem. Soc.* **2002**, *124*, 10552; c) D. E. Elmore, D. A. Dougherty, *J. Org. Chem.* **2000**, *65*, 742.
[7] M. Wojciechowska-Nowak, W. Boczón, U. Rychlewska, B. Warzjtis, *J. Mol. Struct.* **2007**, *840*, 44.
[8] J.-U. Grabow in *Handbook of High-Resolution Spectroscopy* (Eds.: M. Quack, F. Merkt), Wiley-VCH, Weinheim **2010**, Chapter 37.
[9] W. Gordy, R. L. Cook, *Microwave Molecular Spectra*, 3rd ed., Wiley, New York, **1984**.
[10] H. M. Foley, *Phys. Rev.* **1947**, *71*, 747.
[11] J. K. G. Watson in *Vibrational Spectra and Structure, Vol. 6* (Ed.: J. R. Durig), Elsevier, Amsterdam, **1977**, pp. 1–89.
[12] G. T. Fraser, R. D. Suenram, C. L. Lugez, *J. Phys. Chem. A* **2000**, *104*, 1141.
[13] R. Taylor, O. Kennard, *J. Am. Chem. Soc.* **1982**, *104*, 5063.
[14] L. B. Favero, B. M. Giuliano, A. Maris, S. Melandri, P. Ottaviani, B. Velino, W. Caminati, *Chem. Eur. J.* **2010**, *16*, 1761.
[15] G. A. Jeffrey, *An Introduction to Hydrogen Bonding*, Oxford University Press, Oxford, **1997**.
[16] J. E. Perkin, P. J. Buckley, C. C. Costain, *J. Mol. Spectrosc.* **1981**, *89*, 465.
[17] E. J. Cocinero, A. Lesarri, P. Écija, J.-U. Grabow, J. A. Fernández, F. Castaño, *Phys. Chem. Chem. Phys.* **2010**, *12*, 6076.
[18] L. Evangelisti, A. Lesarri, E. J. Cocinero, W. Caminati, J.-U. Grabow, unpublished results.
[19] L. Carballeira, I. Pérez-Juste, *J. Comput. Chem.* **1998**, *19*, 961.
[20] E. L. Eliel, M. Manoharan, *J. Org. Chem.* **1981**, *46*, 1959.
[21] D. J. Hodgson, U. Rychlewska, E. L. Eliel, M. Manoharan, D. E. Knox, E. M. Olefirowicz, *J. Org. Chem.* **1985**, *50*, 4838.
[22] E. L. Eliel, S. H. Wilen, *Stereochemistry of Organic Compounds*, Wiley, New York, **1994**.
[23] F. G. Riddell, *The Conformational Analysis of Heterocyclic Compounds*, Academic Press, New York, **1980**.
[24] S. Blanco, A. Lesarri, J. C. López, J. L. Alonso, *J. Am. Chem. Soc.* **2004**, *126*, 11675.
[25] A. M. Gazaliev, M. Zh. Zhurunov, S. A. Dyusambaev, K. M. Turdybekov, S. V. Lindeman, A. V. Maleev, Yu. T. Struchkov, *Chem. Nat. Compd.* **1990**, *26*, 423.
[26] M. Evain, F.-X. Felpin, C. Laurence, J. Lebreton, J.-Y. Le Questel, *Z. Kristallogr.* **2003**, *218*, 753.
[27] a) Y. Zhao, N. E. Schultz, D. G. Truhlar, *J. Chem. Phys.* **2005**, *123*, 161103; b) Y. Zhao, N. E. Schultz, D. G. Truhlar, *J. Chem. Theory Comput.* **2006**, *2*, 364.
[28] E. G. Hohenstein, S. T. Chill, C. D. Sherrill, *J. Chem. Theory Comput.* **2008**, *4*, 1996.
[29] a) J.-U. Grabow, W. Stahl, *Z. Naturforsch. A* **1990**, *45*, 1043; b) J.-U. Grabow, W. Stahl, H. Dreizler, *Rev. Sci. Instrum.* **1996**, *67*, 4072.
[30] R. D. Suenram, F. J. Lovas, D. F. Plusquellic, A. Lesarri, Y. Kawashima, J. O. Jensen, A. C. Samuels, *J. Mol. Spectrosc.* **2002**, *211*, 110.
[31] Gaussian 03, Rev. E.01, M. J. Frisch, G. W. Trucks, H. B. Schlegel, G. E. Scuseria, M. A. Robb, J. R. Cheeseman, J. A. Montgomery, Jr., T. Vreven, K. N. Kudin, J. C. Burant, J. M. Millam, S. S. Iyengar, J. Tomasi, V. Barone, B. Mennucci, M. Cossi, G. Scalmani, N. Rega, G. A. Petersson, H. Nakatsuji, M. Hada, M. Ehara, K. Toyota, R. Fukuda, J. Hasegawa, M. Ishida, T. Nakajima, Y. Honda, O. Kitao, H. Nakai, M. Klene, X. Li, J. E. Knox, H. P. Hratchian, J. B. Cross, V. Bakken, C. Adamo, J. Jaramillo, R. Gomperts, R. E. Stratmann, O. Yazyev, A. J. Austin, R. Cammi, C. Pomelli, J. W. Ochterski, P. Y. Ayala, K. Morokuma, G. A. Voth, P. Salvador, J. J. Dannenberg, V. G. Zakrzewski, S. Dapprich, A. D. Daniels, M. C. Strain, O. Farkas, D. K. Malick, A. D. Rabuck, K. Raghavachari, J. B. Foresman, J. V. Ortiz, Q. Cui, A. G. Baboul, S. Clifford, J. Cioslowski, B. B. Stefanov, G. Liu, A. Liashenko, P. Piskorz, I. Komaromi, R. L. Martin, D. J. Fox, T. Keith, M. A. Al-Laham, C. Y. Peng, A. Nanayakkara, M. Challacombe, P. M. W. Gill, B. Johnson, W. Chen, M. W. Wong, C. Gonzalez, J. A. Pople, Gaussian, Inc., Wallingford CT, **2004**.

Received: April 5, 2010
Published online: July 9, 2010

 © 2010 Wiley-VCH Verlag GmbH & Co. KGaA, Weinheim